Journal of Power Sources 196 (2011) 10461–10464

Contents lists available at ScienceDirect

Journal of Power Sources

journal homepage: www.elsevier.com/locate/jpowsour

Short communication

A novel synthesis of mesoporous carbon microspheres for supercapacitor electrodes

Wei Xiong[a], Mingxian Liu[b], Lihua Gan[a,*], Yaokang Lv[a], Yang Li[a], Liang Yang[a], Zijie Xu[a], Zhixian Hao[a], Honglai Liu[b], Longwu Chen[a]

[a] Department of Chemistry, Tongji University, 1239 Siping Road, Shanghai 200092, PR China
[b] State Key Laboratory of Chemical Engineering and Department of Chemistry, East China University of Science and Technology, 130 Meilong Road, Shanghai 200237, PR China

ARTICLE INFO

Article history:
Received 21 April 2011
Received in revised form 27 July 2011
Accepted 29 July 2011
Available online 4 August 2011

Keywords:
Mesoporous carbon microspheres
Synthesis
Electrochemical properties
Supercapacitor

ABSTRACT

Mesoporous carbon microspheres (MCMs) with the diameters of 0.5–2.0 μm, main mesopore sizes of 2.6–4.0 nm and specific surface areas of 449–1212 $m^2 g^{-1}$ are synthesized by a novel hydrothermal emulsion-activated method. The typical MCMs as electrode materials have a specific capacitance of 157 $F g^{-1}$ at a high current density of 10.0 $A g^{-1}$ in 6 M KOH aqueous solution. The resultant MCMs electrode materials with high current charge and discharge capability in 6 M KOH aqueous solution provide important prospect for electrode materials in supercapacitors which could offer high power density for electric vehicles.

1. Introduction

Due to its low equivalent series resistance (ESR), long charge–discharge life and high power density, supercapacitors also called electrochemical capacitors or ultracapacitors have been considered to be one of the most promising candidates for high power energy source which could be used for portable electronic devices, electric vehicles and so on [1–3]. To date, among various available electrode materials for supercapacitors, porous carbon-based materials, especially activated carbons, are the most commonly used because of their relatively low cost and larger surface areas [4]. Generally, the electrical energy of activated carbons as supercapacitor mainly stored in the form of electrical double-layer capacitance is attributed to the accumulation of charges at the electrode/electrolyte interface. The intrinsically small micropores of activated carbons limit their accessibility to electrolytes during the charge–discharge process, especially when a large loading current density is employed [5]. Therefore, surface areas of micropores cannot be efficiently utilized, leading to undesirable capacitance of carbon electrode materials in electrolyte solution. To overcome the drawbacks of activated carbons, some researchers improve the electrochemical performance by controlling the pore structure of activated carbon and the regularity of pore arrangement. For example, Wu et al. prepared activated carbons with a combination of KOH etching and CO_2 gasification method. The resultant activated carbon electrode materials with high specific surface areas exhibited a capacitance of 165 $F g^{-1}$ in 1.0 M $NaNO_3$ and 197 $F g^{-1}$ in 0.5 M H_2SO_4 aqueous solution between −0.1 and 0.9 V [6]. Moreover, mesoporous carbon materials with large mesopores (>2 nm) were prepared and have been successfully applied for supercapacitors [7–9]. For example, Hsieh et al. prepared mesoporous carbons by an efficient thermal chemical vapor deposition approach. The mesoporous carbons exhibited a capacitance of 140 $F g^{-1}$ at 0.5 $A g^{-1}$ in 1 M KOH aqueous solution [10]. Xia and co-workers used mesoporous carbons prepared by combining surfactant-templating and natural crab shell hard-templating as an electrode material for supercapacitor, which exhibited a capacitance of 152 $F g^{-1}$ at 5 mV s^{-1} in $(C_2H_5)_4NBF_4$/propylene carbonate electrolyte [11].

Carbon microspheres are usually regular spheroids with homogeneous package which can decrease the resistance of the liquids diffusion and hence improve the capacity of the electrode [12]. Moreover, the space between the microspheres can make the electrolyte accessible to the electrodes, which is benefit to the formation of double layer capacity on the carbon/electrolyte interface [13]. Zhao and co-workers used a high-surface-area mesoporous carbon spheres prepared by a dual-templating approach. The resultant mesoporous carbon electrode materials exhibited a capacitance of 97 $F g^{-1}$ at 0.5 $A g^{-1}$ in $(C_2H_5)_4NBF_4$/propylene carbonate electrolyte and 208 $F g^{-1}$ at 0.5 $A g^{-1}$ in 2.0 M H_2SO_4 aqueous solution [14].

* Corresponding author. Tel.: +86 21 65982654x8430; fax: +86 21 65982287.
E-mail address: ganlh@tongji.edu.cn (L. Gan).

0378-7753/$ – see front matter © 2011 Elsevier B.V. All rights reserved.
doi:10.1016/j.jpowsour.2011.07.083

In this work, we report the synthesis of mesoporous carbon microspheres (MCMs) by employing a hydrothermal emulsion-activated method. The resultant MCMs have the diameters of 0.5–2.0 μm and mesopore sizes of 2.6–4.0 nm. The typical MCMs electrode materials have a specific capacitance of 157 F g^{-1} at a high current density of 10.0 A g^{-1} in 6 M KOH aqueous solution. The high current charge and discharge capability provide important prospects for MCMs to be used as electrode materials in supercapacitors.

2. Experimental

10.0 g of liquid paraffin (ρ = 0.838 g cm^{-3}, oil phase), 2.4 g of sorbitan monooleate (Span 80) and 3.2 g of polysorbate 80 (Tween 80) (emulsifiers) were placed in a 50 mL Teflon-lined autoclave. 9.3 g of resorcinol and 12.1 g of formaldehyde were dissolved in 5 mL deionized water. The resorcinol and formaldehyde aqueous solution acted as the water phase. An oil-in-water (O/W) emulsion was obtained by slowly adding the water phase into the oil phase contained emulsifiers under stirring. The Teflon-lined autoclave was heated at 473 K for 5 h and then was cooled to room temperature. The sample was collected by filtration, washing with water and ethanol, and drying at 373 K for 24 h. The dried samples were carbonized at 1273 K with a heat rate of 278 K min^{-1} in a purified N_2 flow to obtain carbon materials. The obtained carbons were mixed with KOH, and then they were heated to 1273 K under nitrogen atmosphere to prepare MCMs (the final products were labeled as MCMs-x, in which the x denotes the mass ratio of KOH to carbons).

Scanning electron microscopy (SEM) observation was taken in JSM-6700F equipment. N_2 adsorption and desorption isotherms was obtained at 77 K using Micromeritics Tristar 3000 gas adsorption analyzer. The pore size distribution was estimated by Barrett–Joyner–Halenda (BJH) model. The electrochemical measurements were done in electrolyte of 6 M KOH using a three-electrode system in CHI 660D instruments. Hg/HgO electrode was used as a reference electrode (the inner solution is 1 M KOH aqueous solution), and nickel foil as a counter electrode. The working electrode was prepared as follows: First, MCMs (80 wt.%), graphite (10 wt.%), polytetrafluoroethylene (PTFE, 10 wt.%) binder and the required amount of ethanol were mixed thoroughly to form the paste. Second, the thickness chip of 1 or 2 mm was obtained by pressing the paste with a double roller machine. Then the circle electrode chip was intercepted on sheet with the puncher, after drying it under an infrared lamp, the resulting circle electrode chip was pressed onto the nickel foil at a pressure of 20 MPa for 10 s. Then the electrode was dried overnight at 373 K for cyclic voltammetry, galvanostatic charge–discharge and the impedance spectra (frequency range is between 1 mHz and 10^3 kHz) test.

3. Results and discussion

Fig. 1 shows SEM image of typical sample MCMs-3. The MCMs-3 has regular sphere shape with diameters of 0.5–2.0 μm. Besides, macropores are visible in the SEM image, which results from the removal of water in the W/O emulsion system. The emulsion system of Span 80–Tween 80/liquid paraffin/water–resorcinol–formaldehyde is an O/W emulsion, the polymerization of which could obtain porous carbons with pores and pore walls [15]. However, carbon microspheres were prepared with hydrothermal treatment of the emulsion system. These microspheres should correspond to the results of a W/O type emulsion polymerization [16]. These results indicate that the emulsion system occur a phase inversion. According to the theory of cohesion, the emulsion structure could be affected by many factors such as the hydrophilic–lipophilic balance (HLB) value, pH value, phase invert temperature, oil/water phase ratio, etc. [17–19]. For example, Liu et al. found that ammonia could cause the O/W emulsion of Span 80–Tween 80/liquid paraffin/water–resorcinol–formaldehyde to occur a phase inversion [16]. Therefore, the original O/W emulsion should undergoes a phase inversion toward a W/O one with the rise of temperature and pressure under the hydrothermal conditions, and finally carbon microspheres were obtained.

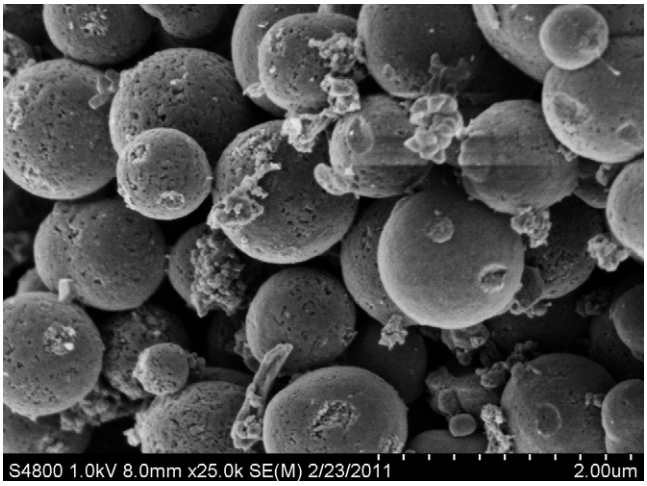

Fig. 1. SEM photograph (25 000×) of MCMs-3.

Fig. 2 shows nitrogen adsorption–desorption isotherms of MCMs-3. The adsorption isotherm is type IV isotherm which has a sharp capillary condensation step at high relative pressures. A hysteresis loop can be observed in the adsorption–desorption isotherms, indicating the existence of mesopore size in MCMs-3. The inset of Fig. 2 shows the pore size distribution curve of MCMs-3 calculated by using the BJH model, and it exhibits single pores with the most probable pore size of 4.0 nm. Generally, KOH often promotes the formation of micropores (<2.0 nm) during the activation process. However, the MCMs prepared by hydrothermal emulsion-activated method exhibited mesopore sizes of 2.6–4.0 nm. For comparison, carbon materials were prepared by emulsion-activated method in the same emulsion system without hydrothermal treatment. The resultant carbons exhibit micropore size of 1.8 nm [20]. Liu et al. prepared mesoporous carbons with pore sizes of 4 nm by using Span 80 as template [21]. In the emulsion system, Span 80 and/or Tween 80 should act not only as emulsifiers, but also as surfactant template during

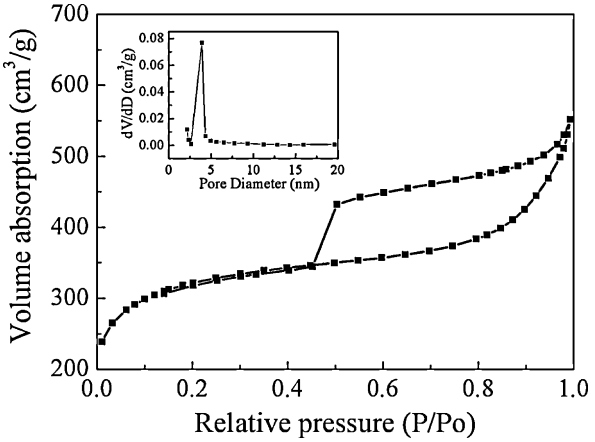

Fig. 2. Nitrogen adsorption–desorption isotherms at 77 K and pore size distribution curve of MCMs-3 (inset).

Table 1
The pore structure parameters of MCMs.

Sample	S_{BET} ($m^2\,g^{-1}$)	S_{mi} ($m^2\,g^{-1}$)	S_{me} ($m^2\,g^{-1}$)	P (nm)	V_{mi} ($m^3\,g^{-1}$)	V_t ($m^3\,g^{-1}$)
MCMs-2	803	732	70	2.6	0.351	0.491
MCMs-3	1010	522	488	4.0	0.283	0.853
MCMs-4	1212	636	576	3.6	0.319	0.854
MCMs-5	668	436	232	3.5	0.257	0.535
MCMs-6	449	289	160	3.0	0.196	0.274

S_{BET}, the specific surface area; S_{mi}, the micropore specific surface area; S_{me}, the mesopores specific surface area; P, the average pore size; V_{mi}, the microporous volume; V_t, the total volume.

hydrothermal conditions. Therefore, the prepared MCMs samples possess relative large mesopores. Table 1 summarizes the textural properties of MCMs samples prepared with different weight ratio of KOH/carbon. The MCMs have specific surface areas of 449–1212 $m^2\,g^{-1}$, total pore volumes of 0.274–0.854 $cm^3\,g^{-1}$ and mesopore sizes of 2.6–4.0 nm. The specific surface areas and total pore volumes of MCMs were enlarged with increasing the KOH/carbon ratio from 2:1 to 4:1, but the pore size increased from 2.6 to 4.0 nm firstly and after slightly declined to 3.6 nm. This should be due to the interior etching process of KOH activation [22]. However, these textural characteristics decreases when the KOH/carbon ratio reaches 5:1 and 6:1 because of the over reaction of KOH with carbons [23].

The bigger pore size is beneficial to the accesses of electrolyte into the pores and consequent ionic transportation for supercapacitors [14]. MCMs-3 and MCMs-4 have relatively larger pore sizes than other samples shown in Table 1. Besides, MCMs-3 and MCMs-4 also have relatively higher specific surface areas. Therefore, we supposed they should possess better electrochemical performance. Fig. 3a shows cyclic voltammogram curves of MCMs-3 and MCMs-4 electrodes at a scan rate of 10 mV s^{-1} in 6 M KOH aqueous solution. It can be observed that MCMs-3 and MCMs-4 electrodes present a nearly perfect quasi-rectangular voltammogram shape, which indicates that these two carbon materials have good electrochemical properties. Besides, MCMs-3 electrode possesses the bigger inner integrated area than MCMs-4, indicating that the specific capacitance of MCMs-3 is much larger than that of MCMs-4. As the scan rate increases, CV curves for MCMs-3 electrode material become some tilted but still maintain a rectangular-like shape (even at a scan rate of 200 mV s^{-1}), as shown in Fig. 3b. This result indicates that a fast charge–discharge process exists in MCMs-3 and the MCMs-3 as electrode materials have high power capability in 6 M KOH aqueous solution [24,25].

The impedance spectrums of MCMs-3 and MCMs-4 electrode materials in 6 M KOH aqueous solution at the potential of −0.8 V are shown in Fig. 4. In the low frequency region, the impedance plot increases with a nearly vertical line, indicating a good capacitive performance. The intermediate frequency region is the 45° line, which is the characteristic of ion diffusion into the electrode materials. The high frequency semicircle reflects the internal resistances of the electrode materials. It can be seen that the internal resistances of MCMs-3 and MCMs-4 electrode materials in 6 M KOH aqueous solution is relatively low. In addition, the internal resistance of MCMs-3 is smaller than that of MCMs-4, which suggests that the MCMs-3 electrode has better conductive properties and consequent electrochemical properties. This matches to the results of the cyclic voltammogram curves.

Fig. 5 exhibits galvanostatic charge–discharge curves of MCMs-3 electrodes in 6 M KOH solution at different loading current density. The MCMs-3 electrodes charge–discharge curves between 0.0 V and −1.0 V vs. Hg/HgO with a good inverse proportion at the loading current density of 1.0, 5.0 and 10.0 A g^{-1}, indicating that MCMs-3 possess a good capacitive behavior. Even at a high current density of 10.0 A g^{-1}, there was no observation of obvious voltage drop at the current switches, indicating a quite low resistance of the electrode.

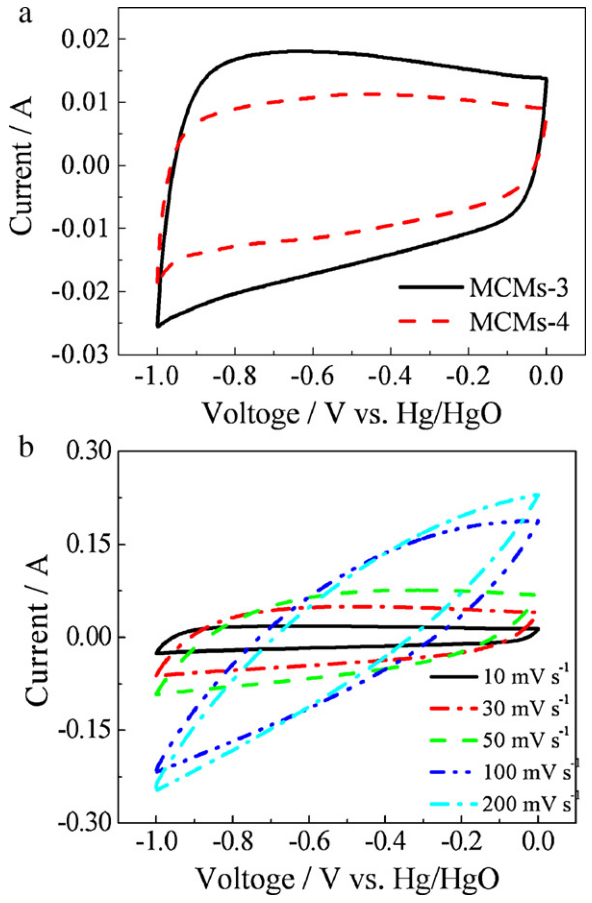

Fig. 3. (a) Cyclic voltammograms of MCMs-3 and MCMs-4 electrodes in 6 M KOH solution at a scan rate of 10 mV s^{-1} and (b) cyclic voltammograms of MCMs-3 electrode in 6 M KOH solution under the different scan rates of 10, 30, 50, 100 and 200 mV s^{-1}.

Moreover, the specific capacitance of MCMs-3 can still remain typical triangle-shaped curves even at a high loading current density of 10.0 A g^{-1}, which reveals that the MCMs-3 as electrode materials suitable for high power application in supercapacitors. The specific capacitance values of the MCMs samples at 1.0 A g^{-1} estimated from charge–discharge curves were shown in Table 2. The specific capacitance of MCMs-3 electrode reaches 171 F g^{-1}, much larger than the other samples including MCMs-4 which has the biggest specific surface areas. Furthermore, the MCMs-3 electrode still exhibits relative high specific capacitance of 157 F g^{-1} at high

Table 2
Capacitance (F g^{-1}) of MCMs samples in 6 M KOH aqueous solution at the loading current density of 1.0 A g^{-1}.

Samples	MCMs-2	MCMs-3	MCMs-4	MCMs-5	MCMs-6
C (F g^{-1})	116	171	126	108	82

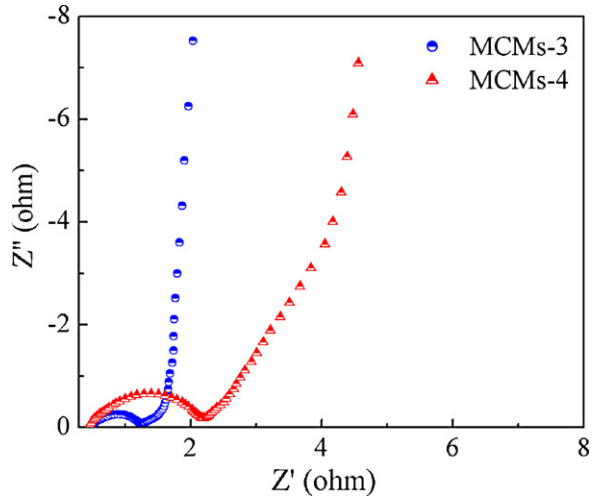

Fig. 4. Nyquist plot of MCMs-3 and MCMs-4 electrodes in 6 M KOH solution measured in the range of 1 mHz to 10^3 kHz.

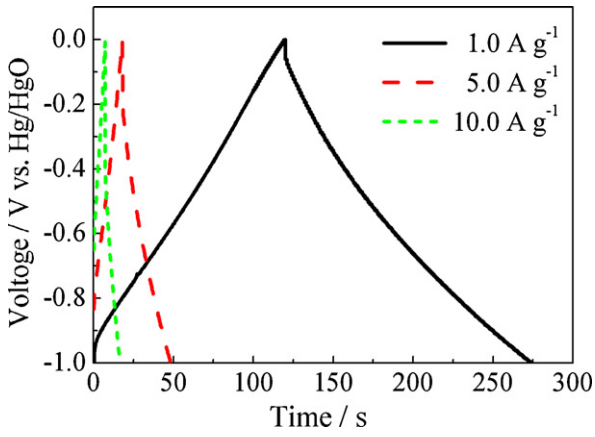

Fig. 5. Charge–discharge curves of MCMs-3 electrode in 6 M KOH solution at the different constant current densities of 1.0, 5.0 and 10.0 A g^{-1}.

current density of 10.0 A g^{-1} with the retention of 92%. Specific energy and specific power of the MCMs-3 electrode materials are 4.89 W h kg^{-1} and 309 W kg^{-1}, respectively, which calculated from charge–discharge curves at the current density of 1.0 A g^{-1} in 6 M KOH aqueous solution. The energy density of the MCMs-3 electrode material is comparative to most of commercial electric double layer capacitor (EDLC) which generally ranges from around 3 to 5 W h kg^{-1} [26].

The good electrochemical properties of MCMs-3 electrode materials could be ascribed to two aspects: high specific surface area and large pore size. On the one hand, the specific surface area of MCMs-3 is as large as 1010 m^2 g^{-1} compared to other samples such as MCMs-2 and MCMs-5. Correspondingly, in 6 M KOH aqueous solution, the specific capacitance of MCMs-3 reaches 171 F g^{-1} at a current density of 1.0 A g^{-1}, much higher that those of MCMs-2 and MCMs-5 which are 116 and 108 F g^{-1}, respectively. On the other hand, the specific surface area of MCMs-3 is smaller than that of MCMs-4, but the specific capacitance of MCMs-3 electrode materials is higher than that of MCMs-4 (126 F g^{-1}) at a current density of 1.0 A g^{-1}. This should be due to that the pore size of MCMs-3 is larger than that of MCMs-4. The larger mesopore size is favorable for ion diffusion throughout MCMs-3, which leads to improved capacitive activity. As a result, MCMs-3 possesses a good electrochemical performance, which provides important candidate as electrode material for supercapacitors.

4. Conclusions

In conclusion, MCMs with the diameters of 0.5–2.0 μm, mesopore sizes of 2.6–4.0 nm and specific surface areas of 449–1212 m^2 g^{-1} were synthesized by a novel hydrothermal emulsion-activated method. A typical sample, MCMs-3 which has high specific surface area of 1010 m^2 g^{-1} and pore size of 4.0 nm as electrode materials exhibits specific capacitance of 171 F g^{-1} at a constant discharge current density of 1.0 A g^{-1} in 6 M KOH aqueous solution. Even at the high current density of 10.0 A g^{-1}, it still possesses relative high specific capacitance of 157 F g^{-1}. The high current charge and discharge capability offer the promising prospects for the application of MCMs-3 as electrode materials in supercapacitors which meet the need of high power density.

Acknowledgments

The project was supported by the National Natural Science Foundation of China (20973127, 20776045 and 20736002), Shanghai Nanotechnology Promotion Center (0952nm00800), the National High Technology Research and Development Program of China (2008AA062302), China Postdoctoral Science Foundation (20090460647 and 2010030258) and Shanghai Postdoctoral Scientific Program (10R21412100).

References

[1] S. Jagannathan, H. Chae, R. Jain, S. Kumar, J. Power Sources 185 (2008) 676–684.
[2] A. Sierczynska, K. Lota, G. Lota, J. Power Sources 195 (2010) 7511–7516.
[3] W. Kim, M. Kang, J. Joo, N. Kim, I. Song, P. Kim, J. Yoon, J. Yi, J. Power Sources 195 (2010) 2125–2129.
[4] D. Qu, J. Power Sources 109 (2002) 403–411.
[5] J. Ndamanisha, Y. Hou, J. Bai, L. Guo, Electrochim. Acta 54 (2009) 3935–3942.
[6] F. Wu, R. Tseng, C. Hu, C. Wang, J. Power Sources 159 (2006) 1532–1542.
[7] C. Yuan, B. Gao, L. Shen, S. Yang, L. Hao, X. Lu, F. Zhang, X. Zhang, Nanoscale 3 (2011) 529–545.
[8] Z. Wen, Q. Qu, Q. Gao, X. Zheng, Z. Hu, Y. Wu, Y. Liu, X. Wang, Electrochem. Commun. 11 (2009) 715–718.
[9] S. Lee, S. Mitani, C. Park, S. Yoon, Y. Korai, I. Mochida, J. Power Sources 139 (2005) 379–383.
[10] C. Hsieh, Y. Lin, Microporous Mesoporous Mater. 93 (2006) 232–239.
[11] H. Liu, X. Wang, W. Cui, Y. Dou, D. Zhao, Y. Xia, J. Mater. Chem. 20 (2010) 4223–4230.
[12] F. Wang, K. Li, Y. Lu, Q. Li, C. Lu, C. Sun, New Carbon Mater. 21 (2006) 219–223.
[13] A. Deshmukh, S. Mhlanga, N. Coville, Mater. Sci. Eng. Rep. 70 (2010) 1–28.
[14] Q. Li, R. Jiang, Y. Dou, Z. Wu, T. Huang, D. Feng, J. Yang, A. Yu, D. Zhao, Carbon 49 (2011) 1248–1257.
[15] M. Liu, L. Gan, F. Zhao, H. Xu, X. Fan, C. Tian, X. Wang, Z. Xu, Z. Hao, L. Chen, Carbon 45 (2007) 2710–2716.
[16] M. Liu, L. Gan, Z. Xu, L. Chen, J. Hu, H. Liu, Chem. Lett. 39 (2010) 274–275.
[17] L. Chen, Y. Shang, H. Liu, Y. Hu, J. Colloid Interface Sci. 301 (2006) 644–650.
[18] T. Dimitrova, F. Leal-Calderon, Langmuir 15 (1999) 8813–8821.
[19] M. El-Aasser, C. Lack, J. Vanderhoff, F. Fowkes, Colloid Surf. 29 (1988) 103–118.
[20] W. Xiong, M. Liu, L. Gan, X. Wang, Z. Xu, Z. Hao, H. Liu, L. Chen, Adv. Mater. Res. 239–242 (2011) 1396–1399.
[21] M. Liu, L. Gan, C. Tian, J. Zhu, Z. Xu, Z. Hao, L. Chen, Carbon 45 (2007) 3042–3059.
[22] R. Tseng, S. Tseng, J. Colloid Interface Sci. 287 (2005) 428–437.
[23] K. Babel, K. Jurewicz, J. Phys. Chem. Solids 65 (2004) 275–280.
[24] F. Wu, R. Tseng, C. Hu, C. Wang, J. Power Sources 138 (2004) 351–359.
[25] C. Huang, Y. Wu, C. Hu, Y. Li, J. Power Sources 172 (2007) 460–467.
[26] B. Xu, F. Wu, S. Chen, Z. Zhou, G. Cao, Y. Yang, Electrochim. Acta 54 (2009) 2185–2189.